

# Estimating Censored Spatial-Temporal Demand with Applications to Shared Micromobility

Alice Paul

alice\_paul@brown.edu, Brown University

Kyran Flynn

kyran.flynn@brown.edu, Brown University

Cassandra Overney

overney@mit.edu, Massachusetts Institute of Technology

March 20, 2023

## Abstract

In shared micromobility networks, such as bike-share and scooter-share networks, operators and city planners are interested in understanding user demand. However, observed trips do not equate directly to demand. The distribution of available bikes affects the distribution of observed trips both through the censoring of potential users who cannot find a nearby bike and the spatial dependence between where a user originates and where a trip begins. The ability to use trip data to accurately estimate demand in both docked and dockless systems is key to analyze the number of dissatisfied users, operational costs, and equity in access, especially for city officials. In this paper, we present a flexible and interpretable framework to estimate spatial-temporal demand by explicitly modeling how users interact with the system. This choice model and algorithm was informed by our collaboration with city planners from Providence, RI, and we demonstrate our algorithm on data from Providence’s dockless scooter-share network. Our estimation algorithm is publicly available to use through an efficient and user-friendly application designed for other city planners and organizations to help inform system planning.

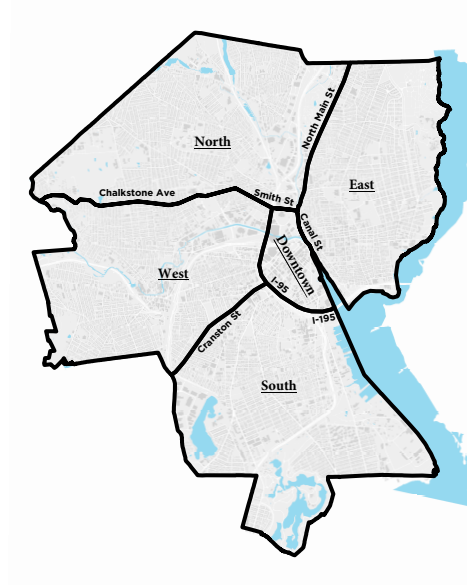
## 1 Introduction

Shared micromobility networks, including bike-share and scooter-share networks, are becoming an established part of urban environments. Access to these networks expands the modes of transportation available and enables connections to existing public transportation. When checking in or checking out a bike or scooter, users directly impact the state of the system and the distribution of available vehicles. This leads to a wealth of individual-level data that city officials can use to extract usage patterns, understand how the population interacts with the network, and inform contracts with the available operators to better serve the city.

While initial shared micromobility networks had a docked structure in which users checked in and out bikes at a set of available stations, more recently there has been an increase in dockless and hybrid systems in which users can return a bike or scooter anywhere by simply checking it

back in through the mobile app and enabling the locking mechanism. Dockless systems increase the flexibility and efficiency of the network [2, 17], allowing the state of the system to adapt to demand. In theory, this leads to increased equity in access. However, there are additional challenges as operators tend to prioritize repositioning scooters or bikes to areas with low idle times over maintaining access across the service area [2, 17]. This makes it even more important for city officials to understand how availability is affecting observed demand to inform the regulations on operators, which can vary significantly between cities. For example, the City of Providence requires each operator to have at least 5% of trips occur in each of five designated regions, shown in Figure 1 [4].

Figure 1: Service regions for Providence’s Shared Micromobility Program [4].



Because availability affects demand itself, equitable access can be defined as availability that is correlated with the true underlying demand when there is dependable and nearby access. This underlying demand naturally varies across the service area given the underlying population (e.g. number of commuters or students) and built environment (e.g. distance to public transportation, access to bike lanes) [2]. Therefore, it is important to adjust for censoring due to unavailability when estimating demand from past usage — the observed data will not contain events for users who wanted to use the system but did not find an available bike or scooter. In this paper, we present a new framework for estimating spatial-temporal demand from past usage using an Expectation-Maximization (EM) algorithm to estimate the underlying parameters. Our demand estimation algorithm incorporates a probability model on whether a user at a particular location will find an available bike or scooter to explicitly model the observed censoring. Additionally, this model extends to both docked and dockless system by directly incorporating the spatial dependence and censoring on a user’s initial location. Estimating user location through this choice model is important because this data is not generally made available to city officials.

To illustrate the use of our algorithm, we present a specific user choice model based on the

distance between an arriving user and the available scooters or bikes. This model can be specified by two interpretable parameters, but our algorithm can be extended to other user choice models. Our estimation algorithm is incorporated into a publicly available application that allows users to efficiently analyze their own data. Additionally, because the output from the algorithm is a matrix of estimated rates of arrival by location and time, the application visualizes this distribution for the user and highlights areas with potential unmet demand. By focusing on the usefulness and ease of interpretation, we hope to increase the audience for these tools and allow more people without data analysis training to gain insight from publicly available data.

In Section 2, we place our work in the context of past literature on estimating demand in shared micromobility networks. We then introduce our general framework and user choice model in Section 3 and present our estimation algorithm in Section 4. In Section 5, we demonstrate the use of our publicly available tool using data from Providence, Rhode Island and comment on the results. Additionally, a small test data set, modified from Kansas City’s Microtransit network [3], is available for users to test our application. Last, in Section 6, we perform sensitivity analysis on both a simple simulated example and the Providence data. While our tool gives useful insight into usage patterns and highlights potential areas to increase service levels, future work will focus on how to use the results from this estimation to explicitly analyze how changing access affects user behavior and overall observed demand. We discuss these possible extensions in Section 7.

## 2 Literature Review

Initial research in analyzing bike-share data focused on estimating demand in a docked system. In these cases, the demand at station  $j$  is often modeled as a Poisson arrival process where the arrival rate at station  $j$  in time period  $t$  is given by the number of trips observed during that time period divided by the proportion of time at least one bike was available [9, 10]. The latter part adjusts the estimate to account for potential censoring. In a related paper, [11] introduce a censored likelihood function within a Gaussian process model. However, these estimates ignore the spatial dependence between stations, which can often be quite close together. When one station does not have available bikes, users may choose a nearby station.

In docked systems, another stream of research has focused on predicting trips. These have ranged from regression-based methods [6, 19] to simulation-based methods [20]. To incorporate spatial dependence, some of these methods have used clustering to define neighborhoods to predict the number of trips or trip destinations [5, 8]. More recently, machine learning methods such as gradient-boosted regression trees [13] and attention-based networks [18, 21] have also been applied to improve prediction of trips in docked systems. Additionally, researchers have focused on using the demand estimates above to inform decisions such as placement and redistribution of bikes [9, 10].

Dockless systems bring additional flexibility to users and require different methods to predict demand and usage. A dockless system also allows operators to adjust availability without having to change the station structure. This leads to the potential for increased equity [17, 2]. However, there is also potentially large overestimation of service levels when censoring is not considered given the spread of availability [1].

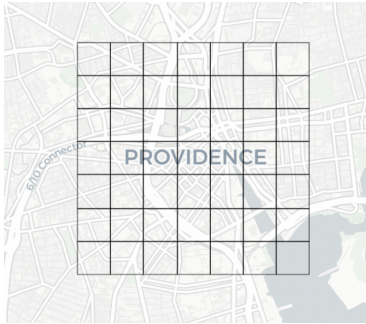
Predicting trips or demand in dockless systems requires a spatial-temporal representation of the system such as representing the network as a grid or graph. Models predicting trips have incorporated this structure and utilized different machine learning methods such as random forests

[24], gradient boosted decision trees [15], convolutional neural networks [22], and long short-term memory neural networks [23, 14]. The complexity of these methods increase prediction accuracy but give less informative outcomes to city planners. [12] aims to find a sparse representation of the travel between different regions in the service area. To our knowledge, there has been limited work on directly estimating demand in dockless systems beyond using the grid system to have each grid point represent a ‘station’ and applying the methods mentioned above [1]. This again ignores the spatial dependence between grid points. While we also use a grid to represent the service area, this paper directly models users arriving in one cell and choosing a bike or scooter in another grid cell, meaning that as we decrease the size of each grid cell we can estimate a very granular picture of demand.

### 3 Framework and User Choice Model

In this section, we define our general framework and our model for how users arrive and make decisions. For ease of presentation, we consider our shared micromobility network to only have available bikes. We first discretize the space by inducing a grid  $\mathcal{G}$  over the network and indexing the grid cells  $i = \{1, 2, \dots, m\}$ . Further, we discretize the times of day into discrete time periods  $t = 1, 2, \dots, \mathcal{T}$ . In our app, these time periods are set to the hours of the day and the granularity of this grid is specified by the user — smaller grid cells give more detailed demand estimates but require more computation time.

Figure 2: Visualization of blank grid discretization (400m grid cells, Providence).



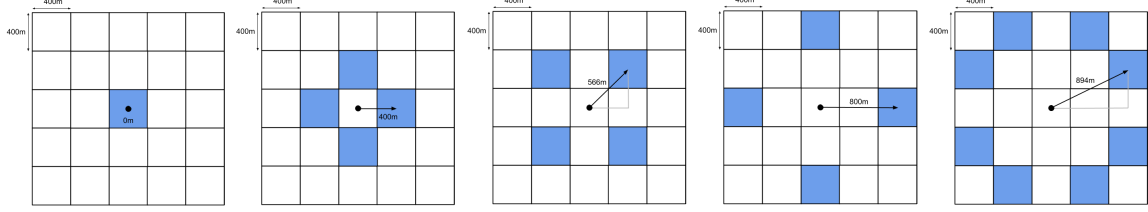
Our framework makes the following three assumptions.

1. All bikes and users are located at the center point of the corresponding grid cell.
2. For each time period  $t = 1, 2, \dots, \mathcal{T}$  and grid cell  $i \in \{1, 2, \dots, m\}$ , users arrive in the center of grid cell  $i$  following an independent Poisson process with rate parameter  $\mu_{t,i}$ .
3. Each arriving user  $j$  observes the available demand and either picks a bike from grid cell  $i \in \{1, 2, \dots, m\}$  with probability  $\text{prob}_i$  or leaves the system without using a bike with probability  $\text{prob}_0$ , where  $\text{prob}_0 + \sum_{i=1}^m \text{prob}_i = 1$ . If a user decides to choose a bike from grid cell  $i$ , they choose one at random from the available bikes in that cell.

The framework above assumes that the rate  $\mu_{t,i}$  is fixed for each time period and grid cell. That is, that the variance in actual demand can be accounted for by the estimated Poisson distribution



Figure 3: Visualization of relative grid cell distances in a 400m grid with a maximum distance of 1000m.



itself. Dependency on other covariates such as the day of week, season, or other characteristics is discussed in Section 4.3. The probabilities  $\text{prob}_i$  incorporate the censoring and spatial dependence between a user’s location and any generated trip. Note that our estimation algorithm is agnostic to the distribution of these probabilities and can be generalized to any choice model. For example, a user choice model may take into account the direction of travel.

We consider a choice model in which users have a threshold distance they are willing to travel from where they arrive to where they pick up a bike. Users then greedily choose an available bike within that threshold, breaking ties randomly. If no bike is within the user’s threshold, they leave without generating a trip. For example, in Figure 3 if a user arrives and has a threshold of 250m, they would only consider bikes within their same grid cell since all other grid cells are at least 400m away.

To model the distribution of user thresholds, we use a discretized version of a half-normal distribution as shown below. In particular, for a half-normal distribution with standard deviation  $\sigma$ , let  $f_\sigma(x)$  be the corresponding cumulative distribution function. We consider all possible distances  $\mathcal{D} = \{\text{dist}_0, \text{dist}_1, \dots, \text{dist}_{\max}\}$  between the center points of two grid cells up to distance  $\text{dist}_{\max}$ , the maximum distance a user would be willing to walk to find a bike, and define the probability a user has a threshold in the range  $[\text{dist}_i, \text{dist}_{i+1})$  to be

$$\Pr(\text{dist}_i \leq \text{threshold} < \text{dist}_{i+1}) := (f_\sigma(\text{dist}_{i+1}) - f_\sigma(\text{dist}_i)) / (1 - f_\sigma(\text{dist}_{\max})).$$

Given the assumption that all bikes and users are located at the center point of a grid cell, this is the probability a user considers bikes up to a distance  $\text{dist}_i$  away. Figure 3 shows how the grid induces the set of possible travel distances, and Figure 4 demonstrates how the folded normal distribution leads to the discretized threshold probabilities for a set maximum distance and  $\sigma$ .

To set  $\sigma$ , we let  $p_0$  be the probability a user is only willing to consider bikes within their own grid cell and use bisection search to find  $\sigma$  such that  $\Pr(\text{dist}_0 \leq \text{threshold} < \text{dist}_1) \approx p_0$ . Specifying a higher  $p_0$  reduces  $\sigma$  and leads to a sharper decrease in probabilities whereas a small  $p_0$  can lead to an almost uniform distribution on threshold up to the maximum distance, showing the flexibility in this distribution. Figure 5 illustrates this for  $p_0 = 0.1$  and  $p_0 = 0.7$ . Our user threshold distribution is informed by past research on user behavior which indicates that a maximum travel distance of 800m or 1000m is reasonable to assume and that users are more likely to use bikes closer to them [25, 7]. The distribution is also easy to visualize and adjust. In our public application,  $\text{dist}_{\max}$  and  $p_0$  are user-specified parameters with default values of 1000m and 0.7, respectively, for a grid with 400m wide grid cells. These default values and our user choice model overall were also informed by our discussions with city planners from Providence.

Figure 4: The truncated probability density function for the folded half normal distribution with variance  $\sigma^2$  is given by the blue curve and the corresponding user threshold distribution is given by the bar plot.

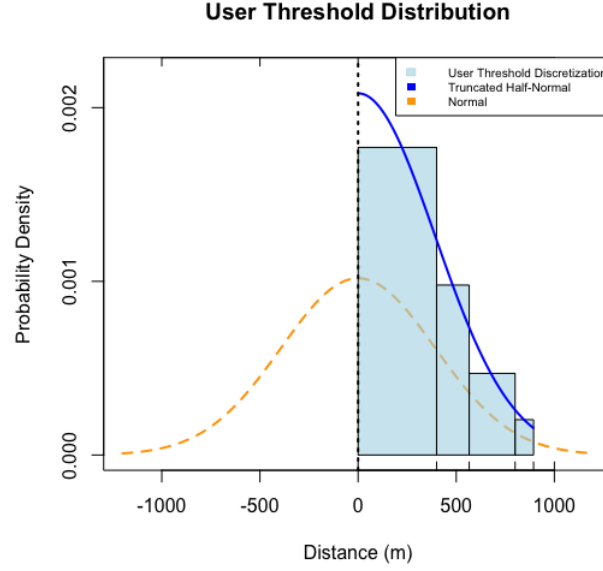
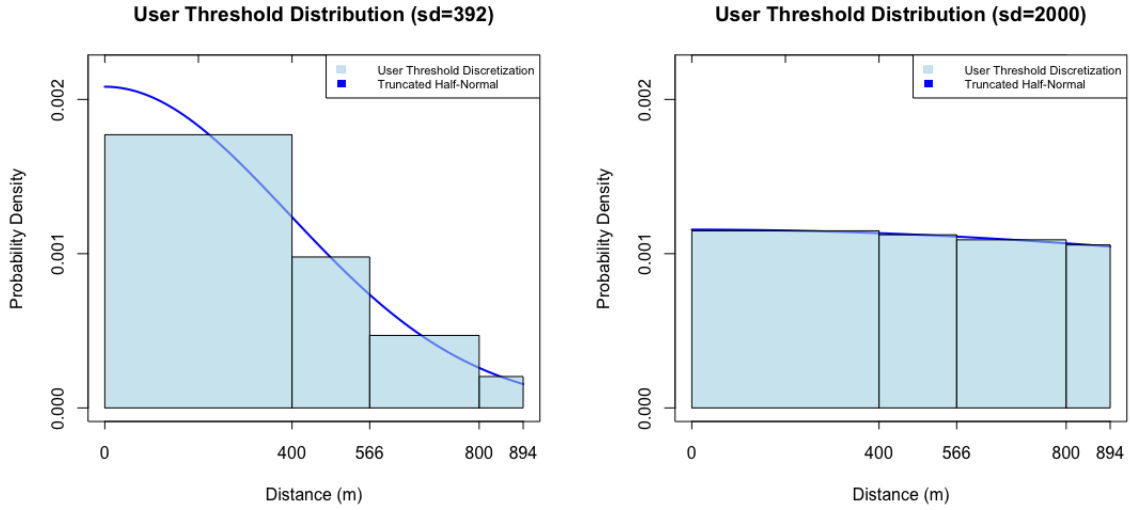


Figure 5: Example of how  $\mathbf{p_0}$  affects the estimated distribution. The user threshold distribution with  $\mathbf{p_0} = 0.7$  ( $\sigma = 392\mathbf{m}$ ) on the left and with  $\mathbf{p_0} = 0.1$  ( $\sigma = 2000\mathbf{m}$ ). A smaller  $\mathbf{p_0}$  shifts the distribution towards a uniform distribution.



## 4 Estimation Algorithm

To estimate the rates  $\mu_{t,i}$ , we assume we have data on the observed trips and the location of available bikes across  $k$  consecutive days indexed by  $d = 1, 2, \dots, k$ . Suppose there are  $n$  observed trips and that each trip  $j = 1, 2, \dots, n$  occurs at cell  $c_j$  in time period  $t_j$  on day  $d_j$ . Our goal is to set  $\mu_{t,i}$  to maximize the likelihood of the observed data. As mentioned, estimating the rates directly from the trips has the following limitations.

1. Users walk from an unobserved cell location to an available bike. Thus, the true location of user demand is not included in the trip origin data.
2. Users may look for a bike and not find one within their user threshold, which is unobserved user demand.

These two limitations require us to back-solve from the data to estimate true demand in each cell. To do so, we define an indicator latent variable  $z_{j,i}$  representing whether the user from the trip  $j$  comes from cell  $i$  and use an algorithm to infer the Poisson arrival rates of each cell during each time period. Before defining the EM algorithm, we define two probabilities necessary for the calculations.

### 4.1 Algorithm Notation

First, we define  $\pi_{j,i}$  to be the probability a user arriving in cell  $i$  at the time of trip  $j$  would choose a bike in cell  $c_j$ , where  $c_j$  is the cell from which trip  $j$  begins. Let  $\text{dist}_{j,i}$  be the distance between grid cell  $i$  and  $c_j$ ,  $S_i$  be the set of bikes closest to grid cell  $i$ , and  $S_{j,i}$  be the set of bikes within grid cell  $c_j$ . There are two cases.

1. There exists another available bike in a cell closer to  $i$  than  $c_j$ . That is,  $S_{j,i} \not\subseteq S_i$ . In this case, we have  $\pi_{j,i} = 0$ .
2. The bikes in grid cell  $c_j$  are part of the set of closest bikes to the user. Then the probability a user in grid cell  $i$  would choose a bike in grid cell  $j$  is based on whether the user's threshold is at least  $\text{dist}_{j,i}$  and the fraction of bikes in  $S_i$  that are in grid cell  $c_j$ .

$$\pi_{j,i} = \Pr(\text{threshold} \geq \text{dist}_{j,i}) \frac{S_{j,i}}{S_i}.$$

Second, we define  $\alpha_{t,i}$  to be the probability a user arriving in cell  $i$  at a uniformly distributed time within time period  $j$  and with a random threshold will find a bike within their distance threshold. To estimate this probability, we consider each possible threshold value range. Suppose that the user's threshold is in the range  $[\text{dist}_l, \text{dist}_{l+1})$  and consider the availability during time period  $t$ . Using the bike locations during that time period, we can find the percent of time that the closest bike to cell  $i$  is at most relative cell distance  $\text{dist}_l$  away from cell  $i$ . Let this value be  $\text{perc}_{t,i,l}$ . Then, to find  $\alpha_{t,i}$ , we consider all possible ranges for the user's threshold. Summing these probabilities over all feasible distances and then averaging across the days, we obtain an empirical estimate for  $\alpha_{t,i}$ .

$$\hat{\alpha}_{t,i} = \sum_{l=0}^{|\mathcal{D}|-1} \text{perc}_{t,i,l} \cdot \Pr(\text{dist}_l \leq \text{threshold} < \text{dist}_{l+1}).$$

## 4.2 EM Algorithm

As mentioned earlier, we introduce the indicator latent variable  $z_{j,i}$  representing whether the user from trip  $j$  comes from cell  $i$ . Since each trip can come from only one cell, we have the constraint that  $\sum_{i=1}^m z_{j,i} = 1$ . We now consider the full data  $(x, z)$  where  $x$  is the observed trip data  $x$  and  $z$  is the unobserved data. The log-likelihood of the observed data with arrival rates  $\mu$  can be written as

$$\begin{aligned}\ell(\mu; x) &= \sum_{j=1}^n \log p(c_j | \mu) \\ &= \sum_{j=1}^n \log \sum_{i=1}^m p(c_j, z_{j,i} = 1 | \mu)\end{aligned}$$

We use an EM algorithm to maximize the log-likelihood function by alternating between two steps: an Expectation Step (E-Step) and a Maximization Step (M-Step). In the E-Step, we maximize the expectation of log-likelihood with respect to the latent indicator variables  $z$  given the data  $x$  and current estimates for  $\mu$ , and in the M-Step, we maximize the log-likelihood estimate with respect to the parameters  $\mu$  given the data  $x$  and the current probability estimates for  $z$ . The algorithm is guaranteed to converge to a local optima [16].

In the expectation step of the algorithm, we maximize the log-likelihood with respect to the distribution of  $z$  given  $x$  and  $\mu$ . Since

$$p(c_j, z_{j,i} = 1 | \mu) = p(z_{j,i} = 1 | c_j, \mu) \cdot p(c_j | \mu)$$

we can maximize the log-likelihood by estimating the first term, the posterior probability that  $z_{j,i} = 1$  given the data and arrival rates  $\mu$ . Now  $p(z_{j,i} = 1 | c_j, \mu)$  is the probability that the user from the  $j^{th}$  trip starting in cell  $c_j$  during time period  $t_j$  comes from cell  $i$ . We'll define this likelihood to be the membership weight of trip  $j$  to cell  $i$   $w_{j,i}$ , which can be derived as follows.

Given a mixture of  $m$  independent Poisson processes with average rates  $\mu_{t_j,1}, \mu_{t_j,2}, \dots, \mu_{t_j,m}$  during time period  $t_j$ , the probability that a user is from Poisson process  $i$  is given by  $\mu_{t_j,i} / \sum_{l=1}^m \mu_{t_j,l}$ . Using the probability  $\pi_{i,j}$  that an arriving user in cell  $i$  at the time of the trip  $j$  chooses the bike from trip  $j$  in cell  $c_j$ , we find that the overall probability is given by

$$\pi_{i,j} \cdot \frac{\mu_{t_j,i}}{\sum_{l=1}^m \pi_{l,j} \mu_{t_j,l}}.$$

We then normalize this probability distribution over all cells to obtain the likelihood membership weights  $w_{j,i}$ .

$$w_{j,i} = \frac{\left( \frac{\pi_{i,j} \mu_{t_j,i}}{\sum_{l=1}^m \pi_{l,j} \mu_{t_j,l}} \right)}{\sum_{i'=1}^m \left( \frac{\pi_{i',j} \mu_{t_j,i'}}{\sum_{l=1}^m \pi_{l,j} \mu_{t_j,l}} \right)} = \frac{\pi_{i,j} \mu_{t_j,i}}{\sum_{i'=1}^m \pi_{i',j} \mu_{t_j,i'}} \quad (1)$$

Intuitively, the membership weights balance the arrival rates by the likelihood a user would actually travel to cell  $j$  from cell  $i$ .

In the maximization step of the EM algorithm, we maximize the estimate for log-likelihood with respect to  $\mu$  given the data and the current distribution of  $z$  found in the E-Step. Estimating the

likelihood as  $p(c_j, z_{j,i} = 1|\mu) = p(z_{j,i} = 1|c_j, \mu) \cdot p(c_j|z_{j,i} = 1, \mu)$ , we get

$$\hat{\mu} = \sum_{j=1}^n \log \sum_{i=1}^m w_{j,i} p(c_j|z_{j,i} = 1, \mu).$$

Since the arrivals in cell  $i$  follow a Poisson distribution, given a fixed number of arrivals, the distribution of those arrivals over time period  $t$  is uniformly distributed. Recall the probability  $\alpha_{t,i}$  that a uniformly distributed user arriving in cell  $i$  during time period  $t$  finds a bike within their threshold. Then the number of observed points follows a Poisson distribution with mean  $\alpha_{t,i} \cdot \mu_{t,i}$ . Therefore, setting  $\mu_{t,i}$  to maximize the likelihood of observing  $x$  will yield estimate

$$\hat{\mu}_{t,i} = \frac{\frac{1}{k} \sum_{j:t_j=t} \hat{w}_{j,i}}{\hat{\alpha}_{t,i}}, \quad (2)$$

where  $\hat{w}_{j,i}$  is calculated using Equation 1 using the current estimate of  $\hat{\mu}$ .

In summary, we can find estimated rates  $\hat{\mu}$  by alternating between the following two steps.

1. E-Step: Maximize the expectation of log-likelihood with respect to the latent indicator variables  $z_j$  given the data  $x$  and current arrival rates  $\hat{\mu}$  by using Equation 1 to update the estimated membership weights  $\hat{w}_{j,i}$ .
2. M-Step: Maximize the log-likelihood estimate with respect to the parameters  $\mu$  given the data  $x$  and the current membership weights  $\hat{w}_{j,i}$  by using Equation 2 to update the estimated arrival rates  $\hat{\mu}_{t,i}$ .

### 4.3 Extensions

We conclude this section by describing extensions to the above framework. In Section 3, we assumed the Poisson arrival rates are fixed from day to day. If we want to allow certain factors to impact arrival rates such as the weather, season, or day of the week, we can either filter the data prior to analysis or the model can be extended to estimate a rate  $\hat{\mu}_{t,i}$  for each day by allowing for a weighted average in the M-step, with weights reflecting the similarity between days using the specified characteristics. Additionally, the model can be extended to predict demand for trips rather than just starting location by using the distribution of drop-off locations. Drop-off locations have the added benefit of being uncensored in the case of dockless systems. Last, the algorithm above is also flexible enough to extend beyond bike-share or scooter-share programs to any settings in which we are interested in estimating rates of events where the observed events depend on some underlying availability. For example, it could be used to model demand for bus travel routes when users may switch between buses depending on the schedule and time of day.

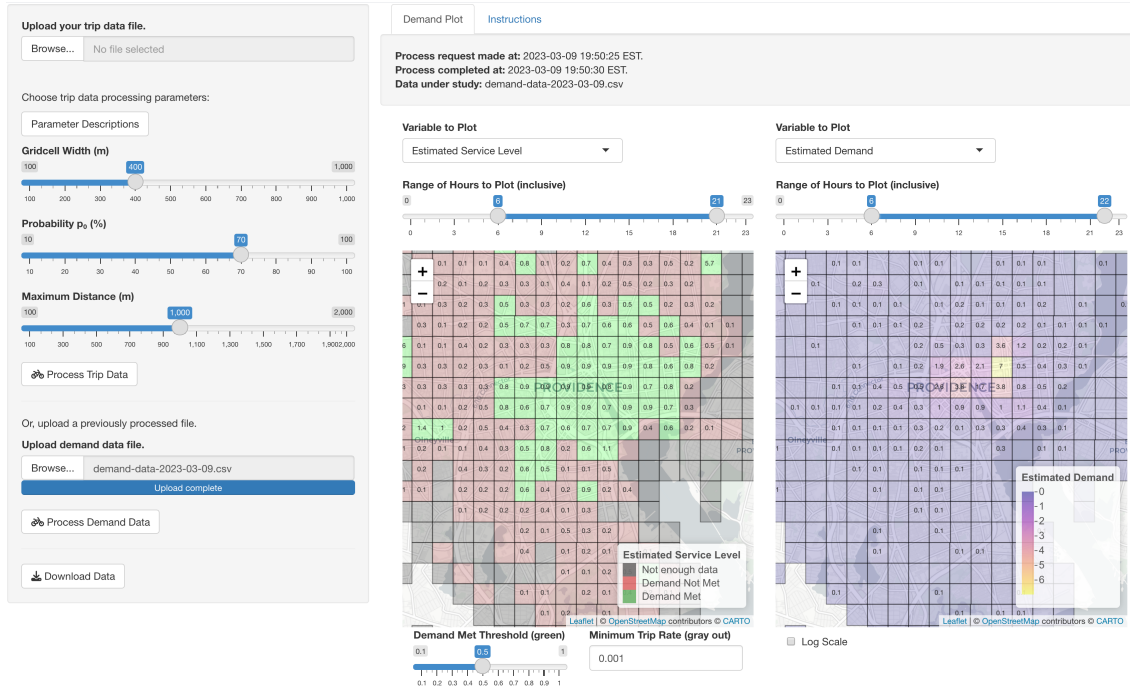
## 5 Implementation, Public Application, and Example

Our code is available to use through a live R Shiny application. The demand estimation algorithm was implemented in python 3.10.9. The grid discretization of the map is incorporated through a grid object, which keeps track of the set of grid cell objects it contains. Each grid cell is efficiently indexed by the grid, and keeps track of its location and nearby bike availability. A data processing class then parses the input trip data sequentially to simultaneously update the relative grid cell availabilities

of the grid, and use the grid cells' availability values to compute the appropriate  $\pi$  and  $\alpha$  values. Once computed, the  $\pi$  and  $\hat{\alpha}$  values are fed into an EM class to iteratively update the estimated membership weights  $\hat{w}$  and arrival rates  $\hat{\mu}$  until a stable set of demand rates  $\hat{\mu}$  is obtained or a set number of iterations is reached. Our code is available at <https://github.com/KyFlynn/shared-mobility-research>.

To create a user-friendly interaction with our model and to visualize the results, we host a live R Shiny application that communicates with our python demand model through the reticulate package. The app allows users to easily upload their cleaned trip data, select the demand model parameter values of choice (grid cell width, probability  $p_0$ , maximum user distance  $\text{dist}_{max}$ ), and run the model for demand visualization with a click of a button. Once processed, we display side-by-side colored leaflet maps that allow users to analyze and compare the findings of our model in their city. From a drop-down menu, users can choose to visualize the estimated demand rates, the estimated or observed availability, the rate at which trips took place, and a summary visualization that categorizes service levels to highlight where the rate of observed trips is much lower than the estimated demand. These findings allow city planners to determine regions of unmet demand due to low availability not directly inferable from the raw trip data. The data for these findings produced by our model can be downloaded in the app for further data analysis and/or re-uploaded for re-visualization. Our application can be accessed at <https://alicejpaul.shinyapps.io/shared-mobility/>. A local version of the app can also be downloaded through the github repository.

Figure 6: Screenshot of the application visualizing Providence demand data.



For Providence data with approximately 100k trips (200k data points) spanning three months distributed over a 276km<sup>2</sup> (~107mi<sup>2</sup>), with default parameter settings (grid cell width of 400m, probability  $p_0$  of 0.7, maximum walking distance of 1km) our application takes approximately 30s

locally and 2min on our live app.<sup>1</sup> In Table 1, we report the runtime of our app both locally and on the published Shiny app for different grid cell sizes and numbers of trips, keeping all other input parameters equal. Entries without data in the website column mean the website ran out of memory running the demand model. For large amounts of data and/or for high granularity of estimated demand, we recommend downloading the application from the github repo and running it locally.

Table 1: Runtime of our demand model locally versus on our public application for different grid cell sizes and number of trips in input trip data.

Grid Cell Width (m)	Number of Trips	Local Runtime (s)	Website Runtime (s)
200	100k	107	-
	200k	460	-
	300k	871	-
400	100k	34	144
	200k	63	598
	300k	87	-
600	100k	16	44
	200k	32	130
	300k	46	293

## 5.1 Results

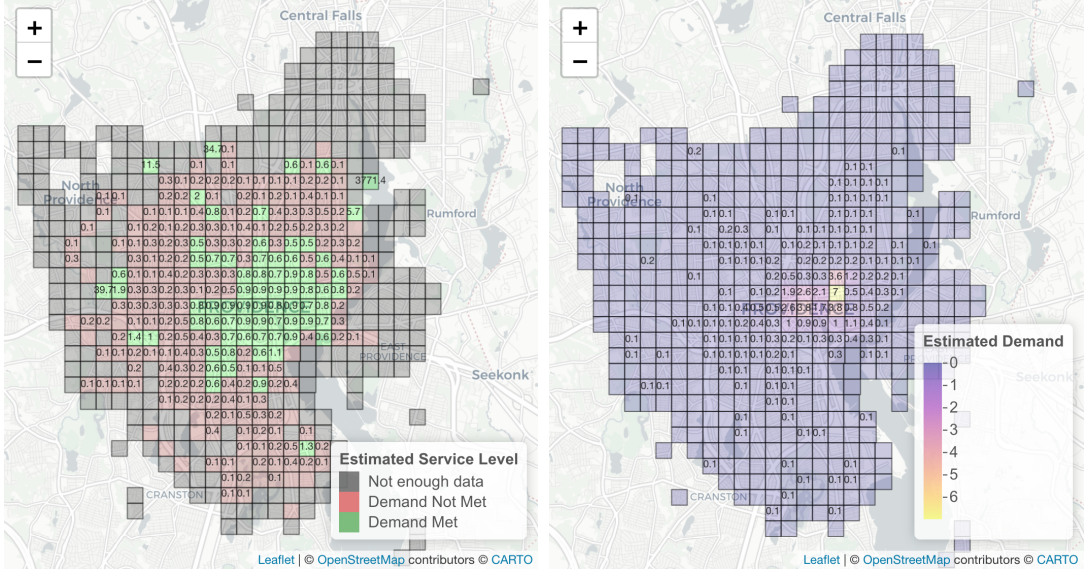
We now present results from scooter data from Providence, RI for June 1, 2019 to August 31, 2019. In Figure 7, the plots display an estimation of the service level and the estimated demand rates  $\hat{\mu}$  averaged over the operating hours (6 am to 10 pm) of the day. The requirement for a grid cell to show up for both of these plots is that the estimated availability  $\hat{\alpha}$  is at least  $10^{-2}$ . Choosing the cutoff service level that estimated demand is at most twice the observed trip rate, we observe that demand is not being met on the outskirts of downtown Providence. On the right, we observe higher estimated demand in downtown Providence and College Hill, as expected, but find that user demand is spread throughout the city.

In Figure 8, the plots display the estimated bike availability  $\hat{\alpha}$  and the observed trip rates. Even with the default value of 0.7 for  $p_0$ , which corresponds to a sharp decrease in acceptance probability with distance, our model estimates availability in much of wider Providence. As expected, we find that most of the trips occur in downtown Providence and College Hill. Overall, the plots together indicate that availability is somewhat extended from these high-demand areas, but that more consistent availability might better serve estimated demand in these areas. Therefore, incorporating estimated availability and demand give important context when considering the distribution of trips.

In our github repository, we have a test data set available for people to try out the application. The trip data was downloaded from Kansas City, MO’s Microtransit Network [3]. We first filter the data to only consider trips from May 1, 2021 to May 6, 2021. The public data does not contain any operator rebalancing. To account for this, we assume perfect rebalancing each day. That is, at the end of each day, bikes are removed and the minimum number needed to ensure the observed

<sup>1</sup>Locally: Apple 2022 16” Macbook Pro, M1 Pro chip: 32GP unified memory; 10-core CPU (8 performance, 2 efficiency); 16-core GPU; 16-core Neural Engine; 200Gbps memory bandwidth.

Figure 7: Visualization of Providence data summer 2019 service level (left) and estimated demand (right).



trips the next day are feasible are relocated. Our R script for processing the data is also available in our repository.

## 6 Sensitivity Analysis

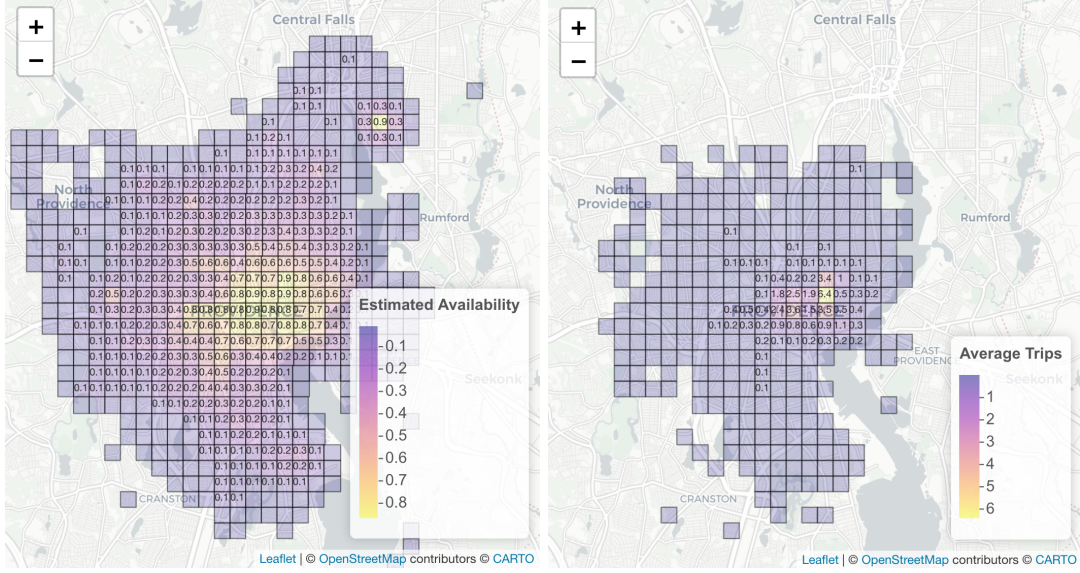
The EM algorithm in Section 4 is guaranteed to converge to a local optima. Therefore, our initial guesses of the rates  $\hat{\mu}$  can impact the returned estimate. We explore this dependence on the Providence data and a simple simulated case. For our simulated data, we generate 50 days of trip data with 10 instantaneous trips per hour starting and ending at the same place in two locations 600m apart longitudinally. Our model creates a small grid of  $7 \times 8$  grid cells around these two active central grid cells, and an initial trip at time zero in both of these cells creates a constant availability of one bike in each of these grid cells for all 50 days. A visualization of the resulting trip rates and estimated availability is given in Figure 9.

For each data set, we consider two extremes: (1) setting the rates uniformly so all grid cells start with the same guess of demand  $\hat{\mu}_{\text{unif}}$  and (2) setting the rates to the average rate of observed trips in that cell and time period  $\hat{\mu}_{\text{trip}}$ . While the former corresponds to an uninformed prior on location the latter ignores any potential travel of users. To analyze the sensitivity of our algorithm to the initial conditions we consider setting the initial  $\hat{\mu}$  values to  $\hat{\mu}_{\gamma} = \gamma \hat{\mu}_{\text{unif}} + (1 - \gamma) \hat{\mu}_{\text{trip}}$  for  $\gamma$  between 0 and 1.

In Figure 11, we plot the largest difference between the  $\mu_{\text{trip}}$  initialization and the  $\mu_{\gamma}$  initialization versus  $\gamma$ . In the simulated data, we observe that the largest difference increases steadily as  $\gamma$  increases, shown in Figure 10. This is expected because we have a limited distribution on availability. As  $\gamma$  increases, the estimated demand spreads from the central cells to the surrounding cells until uniform at  $\gamma = 1$ . Hence, the estimated demand is highly sensitive to the initialization.



Figure 8: Visualization of Providence 2019 summer data estimated availability (left) and trip rates (right).



By contrast, in the Providence data, we observe an immediate increase to a largest difference of around 2, and a subsequent stabilization of the largest difference at this value. The 99th percentile stays relatively low throughout, and the median difference was observed to be 0 for all  $\gamma$ . To generate these results, we did not include grid cells in which estimated  $\hat{\alpha}$  is less than  $10^{-2}$ , the same threshold used in our application. We consider these cells not to have enough availability to infer demand. Note that for regions that did not meet this threshold, the maximum observed difference between  $\hat{\mu}_{\text{trip}}$  and  $\hat{\mu}_{\text{unif}}$  was 103. This is caused by numerical instability in the division by small  $\pi$  and  $\hat{\alpha}$  values in the EM algorithm iterations.

Overall, these results indicate that when we have a more complex and realistic distribution of availability the results are far more robust to our initialization. For this reason, we choose to initialize with  $\hat{\mu}_{\text{unif}}$  in our implementation to avoid biasing the results.

## 7 Future Work

In this paper, we present a flexible and interpretable framework to estimate spatial-temporal demand in the form of estimated Poisson arrival rates. Some possible extensions to this model include incorporating the direction of travel and the built environment into our user choice model. Additionally, the model can be extended to allow the rates to depend on other factors such as day of the week, season, and weather. Last, the results provide insight into user behavior and can be used to inform future decisions such as redistribution and identifying areas with unmet demand. This focus on prescriptive analytics using the estimated model is a promising direction.

Figure 9: Visualization of simulated data trip rates and estimated availability.

0	0	0	0	0	0	0	0										
0	0	0	0	0	0	0	0				0	0	0	0			
0	0	0	0	0	0	0	0			0	0.1	0.3	0.3	0.1	0		
0	0	0	10	10	0	0	0			0	0.3	1	1	0.3	0		
0	0	0	0	0	0	0	0			0	0.1	0.3	0.3	0.1	0		
0	0	0	0	0	0	0	0				0	0	0	0			
0	0	0	0	0	0	0	0										

Figure 10: Visualization of simulated data estimated demand for  $\gamma = \mathbf{0}$ ,  $\gamma = \mathbf{0.5}$ , and  $\gamma = \mathbf{1}$ .

		0	0	0	0				0.3	0.3	0.3	0.3				4.3	4.3	4.3	4.3			
0	0	0	0	0	0	0		0.3	0.3	0.3	0.3	0.3	0.3		4.3	4.3	4.3	4.3	4.3	4.3		
0	0	10	10	0	0			0.3	0.3	9.6	9.6	0.3	0.3		4.3	4.3	4.3	4.3	4.3	4.3		
0	0	0	0	0	0	0		0.3	0.3	0.3	0.3	0.3	0.3		4.3	4.3	4.3	4.3	4.3	4.3		
		0	0	0	0					0.3	0.3	0.3	0.3			4.3	4.3	4.3	4.3			

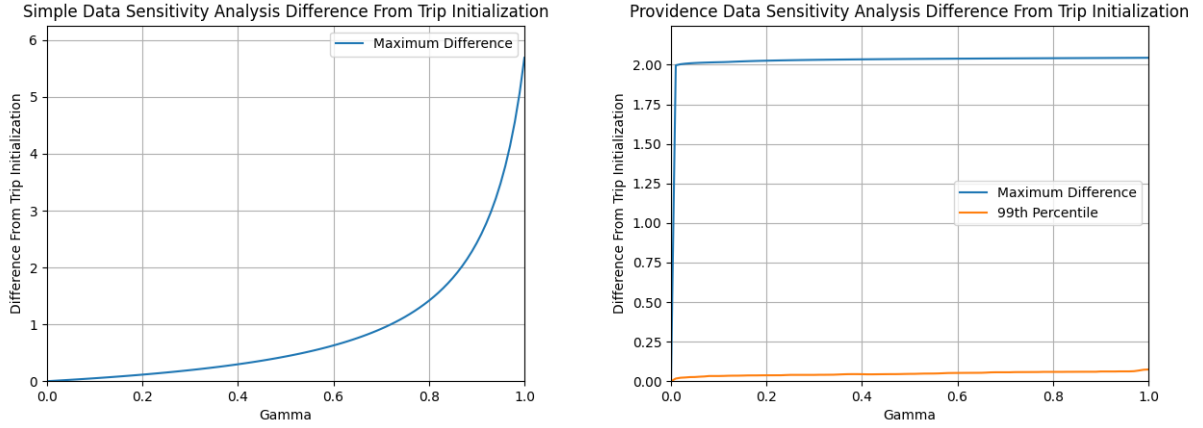
## 8 Acknowledgements

The authors would like to acknowledge principal planner Alex Ellis and curbside administrator Liza Farr with the City of Providence for their help defining our model and framework and their insight into the data and results.

## References

- [1] Szymon Albiński, Pirmin Fontaine, and Stefan Minner. Performance analysis of a hybrid bike sharing system: A service-level-based approach under censored demand observations. *Transportation research part E: logistics and transportation review*, 116:59–69, 2018.
- [2] Zheyang Chen, Dea van Lierop, and Dick Ettema. Dockless bike-sharing systems: what are the implications? *Transport Reviews*, 40(3):333–353, 2020.
- [3] City of Kansas City, MO. Microtransit (scooter and ebike) trips. <https://data.kcmo.org/>

Figure 11: Plot of difference in the estimated demand rates from the trip initialization ( $\gamma = 0$ ) for simple generated data (left) and three months of Providence data (right).



Transportation/Microtransit-Scooter-and-Ebike-Trips/dy5n-ewk5, 2023. Accessed: 2023-03-03.

- [4] City of Providence. Shared micromobility program. [providenceri.gov/planning/e-scooter-share-pilot-program/](https://providenceri.gov/planning/e-scooter-share-pilot-program/), 2023. Accessed: 2023-02-10.
- [5] Pengcheng Dai, Changxiong Song, Huiping Lin, Pei Jia, and Zhipeng Xu. Cluster-based destination prediction in bike sharing system. In *Proceedings of the 2018 Artificial Intelligence and Cloud Computing Conference*, pages 1–8, 2018.
- [6] Cyrille Médard de Chardon and Geoffrey Caruso. Estimating bike-share trips using station level data. *Transportation Research Part B: Methodological*, 78:260–279, 2015.
- [7] Ezgi Eren and Volkan Emre Uz. A review on bike-sharing: The factors affecting bike-sharing demand. *Sustainable cities and society*, 54:101882, 2020.
- [8] Sijia Feng, Hao Chen, Chun Du, Jun Li, and Ning Jing. A hierarchical demand prediction method with station clustering for bike sharing system. In *2018 IEEE Third International Conference on Data Science in Cyberspace (DSC)*, pages 829–836. IEEE, 2018.
- [9] Daniel Freund, Shane G Henderson, Eoin O’Mahony, and David B Shmoys. Analytics and bikes: Riding tandem with motivate to improve mobility. *INFORMS Journal on Applied Analytics*, 49(5):310–323, 2019.
- [10] Daniel Freund, Shane G Henderson, and David B Shmoys. Bike sharing. In *Sharing Economy*, pages 435–459. Springer, 2019.
- [11] Daniele Gammelli, Inon Peled, Filipe Rodrigues, Dario Pacino, Haci A Kurtaran, and Francisco C Pereira. Estimating latent demand of shared mobility through censored gaussian processes. *Transportation Research Part C: Emerging Technologies*, 120:102775, 2020.

- [12] Jingjing Gu, Qiang Zhou, Jingyuan Yang, Yanchi Liu, Fuzhen Zhuang, Yanchao Zhao, and Hui Xiong. Exploiting interpretable patterns for flow prediction in dockless bike sharing systems. *IEEE Transactions on Knowledge and Data Engineering*, 2020.
- [13] Yexin Li, Yu Zheng, Huichu Zhang, and Lei Chen. Traffic prediction in a bike-sharing system. In *Proceedings of the 23rd SIGSPATIAL international conference on advances in geographic information systems*, pages 1–10, 2015.
- [14] Youru Li, Zhenfeng Zhu, Deqiang Kong, Meixiang Xu, and Yao Zhao. Learning heterogeneous spatial-temporal representation for bike-sharing demand prediction. In *Proceedings of the AAAI Conference on Artificial Intelligence*, volume 33, pages 1004–1011, 2019.
- [15] Pengfei Lin, Jiancheng Weng, Song Hu, Dimitrios Alivanistos, Xin Li, and Baocai Yin. Revealing spatio-temporal patterns and influencing factors of dockless bike sharing demand. *IEEE Access*, 8:66139–66149, 2020.
- [16] Geoffrey J McLachlan and Thriyambakam Krishnan. *The EM algorithm and extensions*. John Wiley & Sons, 2007.
- [17] Stephen J Mooney, Kate Hosford, Bill Howe, An Yan, Meghan Winters, Alon Bassok, and Jana A Hirsch. Freedom from the station: Spatial equity in access to dockless bike share. *Journal of transport geography*, 74:91–96, 2019.
- [18] Yan Pan, Ray Chen Zheng, Jiayi Zhang, and Xin Yao. Predicting bike sharing demand using recurrent neural networks. *Procedia computer science*, 147:562–566, 2019.
- [19] Christian Rudloff and Bettina Lackner. Modeling demand for bikesharing systems: neighboring stations as source for demand and reason for structural breaks. *Transportation Research Record*, 2430(1):1–11, 2014.
- [20] Divya Singhvi, Somya Singhvi, Peter I Frazier, Shane G Henderson, Eoin O’Mahony, David B Shmoys, and Dawn B Woodard. Predicting bike usage for new york city’s bike sharing system. In *AAAI Workshop: Computational Sustainability*, 2015.
- [21] Wei Wang, Xiaofeng Zhao, Zhiguo Gong, Zhikui Chen, Ning Zhang, and Wei Wei. An attention-based deep learning framework for trip destination prediction of sharing bike. *IEEE Transactions on Intelligent Transportation Systems*, 22(7):4601–4610, 2020.
- [22] Guangnian Xiao, Ruinan Wang, Chunqin Zhang, and Anning Ni. Demand prediction for a public bike sharing program based on spatio-temporal graph convolutional networks. *Multimedia Tools and Applications*, 80(15):22907–22925, 2021.
- [23] Chengcheng Xu, Junyi Ji, and Pan Liu. The station-free sharing bike demand forecasting with a deep learning approach and large-scale datasets. *Transportation research part C: emerging technologies*, 95:47–60, 2018.
- [24] Zidong Yang, Ji Hu, Yuanchao Shu, Peng Cheng, Jiming Chen, and Thomas Moscibroda. Mobility modeling and prediction in bike-sharing systems. In *Proceedings of the 14th annual international conference on mobile systems, applications, and services*, pages 165–178, 2016.

- [25] Gong Zhang, Hongtai Yang, Shuailin Li, Yi Wen, Yanlai Li, and Fanxiao Liu. What is the best catchment area of bike share station? a study based on divvy system in chicago, usa. In *2019 5th International Conference on Transportation Information and Safety (ICTIS)*, pages 1226–1232. IEEE, 2019.